

Polymorphism of CBr_2Cl_2 ^{†‡}

Maria Barrio,^a Josep Ll. Tamarit,^{*a} Philippe Negrier,^b Luis C. Pardo,^a
Nestor Veglio^a and Denise Mondieig^b

Received (in Montpellier, France) 11th June 2007, Accepted 26th September 2007

First published as an Advance Article on the web 5th October 2007

DOI: 10.1039/b708757h

The polymorphism of dibromodichloromethane (CBr_2Cl_2) has been studied by means of a wide set of experimental techniques as a function of temperature and pressure. From the p - V - T diagram and the derived p - T diagram the volume variations at the transition points have been calculated and compared with those obtained by means of X-ray and neutron powder diffraction. By combining the experimental techniques, it has been demonstrated the existence of a high-pressure orientationally disordered rhombohedral phase ($a^R \approx 14.6 \pm 0.3 \text{ \AA}$ and $\alpha \approx 89.2 \pm 0.2^\circ$). The existence of a glass transition within the monoclinic ($C2/c$, $Z = 32$) low-temperature ordered phase associated with the freezing of exchange positions between Cl and Br atoms is analyzed considering the asymmetry of the intermolecular interactions by means of the study of the thermal expansion tensor. The change of the derivative of the asphericity index, previously reported as a possible “fingerprint” for this kind of glass transitions, is found.

1 Introduction

It is well-known that the behaviour of the outermost electrons of atoms determines the bonding, reactivity and structures of molecules and, thus, of the solids. In general, to reduce the volume of a liquid or a solid by approximately 20%, the GPa region should be reached. Far away, in the megabar region (100 GPa), average interatomic distances can be even decreased by a factor of two.^{1,2}

Probably, one of the major challenges of the solid-state field in this century is not only the understanding of the structural and thermodynamic factors ruling the polymorphism but also the ability to predict the crystalline phases of molecular materials with large technological applications in many domains as pharmaceuticals, organic electronics, or biological systems.

Although the impact of high-pressure studies on new technological applications is enormous,^{3,4} one of the most important aspects is the understanding of the pressure–temperature polymorphism of classic or simple molecular compounds.^{5–7} It should be noticed that most of our physical and chemical knowledge has emerged at or near to atmospheric pressure and effects of the high pressure are still unknown. Of particular interest is the application of high pressure to molecular compounds⁸ and, by increasing complexity, the field of the biochemistry for which biological systems remain still to be

understood under the new variable.⁹ Nevertheless, although high pressure has been used extensively to study materials as metals, semiconductors, superconductors or minerals, organic materials have received rather less attention and it is common to refer to the concept of polymorphism without any comment about the pressure variable.^{10,11} Polymorphism refers to a substance that can adopt more than one crystal structure in the solid state and each one of these different crystalline forms are termed polymorphs. They should correspond to different conditions controlled by pressure and temperature (density being then the dependent variable) and then the pressure–temperature phase diagrams must be mapped over the two “common” variables: pressure and temperature.

Because for some characterized members of the halogenomethane series, $\text{CBr}_{4-n}\text{Cl}_n$, $n = 0, \dots, 4$, the rhombohedral phase has been found at ordinary pressure (CCl_4 , CBrCl_3)^{12–14} we thought that for the CBr_2Cl_2 compound, such a phase should exist before to reach extreme densification conditions, thus without dramatic modifications of the chemical and physical properties. These halogenomethane compounds, in spite of their simple molecular structure, exhibit a number of solid–solid phase transitions.^{15–17} In particular, their globular molecular shape induces for all the elements of the series high-temperature orientationally disordered (OD) or plastic phases, mainly due to the little hindrance for reorientational processes.^{15,16} One of the most interesting experimental facts is that minor changes of the molecular size or symmetry (T_d or C_{3v} or C_{2v}) induced by the change of one of the halogen atoms, produces a fine-tuning in the stability of the different phases. As far as halogenomethanes with T_d molecular symmetry (CCl_4 and CBr_4) are concerned, a high number of experimental and molecular dynamics simulation studies have been published, while for the compounds with lower symmetry (C_{3v} or C_{2v}) only a few experiments have been done.^{18,19} The polymorphism of CBrCl_3 (C_{3v} molecular symmetry) has been studied by several methods such as calorimetry,¹⁵ neutron

^a Departament de Física i Enginyeria Nuclear, E.T.S.E.I.B., Universitat Politècnica de Catalunya, Diagonal, 647 08028 Barcelona, Catalonia, Spain. E-mail: jose.luis.tamarit@upc.edu

^b Centre de Physique Moléculaire, Optique et Hertzienne, Université Bordeaux I-UMR 5798 au CNRS, 351, cours de la Libération, 33405 Talence Cedex, France

[†] Electronic supplementary information (ESI) available: Reflection summary report for Rietveld refinement of CCl_2Br_2 at 220 and 90 K. See DOI: 10.1039/b708757h

[‡] The HTML version of this article has been enhanced with colour images.

Table 1 Transition temperatures T_c and enthalpy (ΔH) changes derived from DSC calorimetric measurements and adiabatic calorimetry from Otha *et al.*¹⁵

Property	Transition				
	$M^S \rightarrow FCC^S$	$FCC^S \rightarrow L^S$	$M^S \rightarrow R^m$	$R^m \rightarrow FCC^S$	$R^m \rightarrow L^S$
T_c / K	258.8 ± 1.0 258.8 ^a	293.7 ± 1.3 294.4 ^a	262.0 ± 2.0^b 262.4 ± 0.9 ^d	243.6 ± 2.0^b 245.6 ± 1.8 ^d	280.7 ± 2.0^b 281.3 ± 1.2 ^d
$\Delta H / kJ mol^{-1}$	5.22 ± 0.24 5.431 ^a	2.30 ± 0.12 2.308 ^a	4.80 ± 0.22^b	0.436 ± 0.08^b	2.36 ± 0.15^b
$\Delta S / J mol^{-1} K^{-1}$	20.2 ± 1.0 21.0 ^a	7.83 ± 0.45 7.84 ^a	18.3 ± 0.90^b	1.79 ± 0.32^b	8.41 ± 0.57^b
$\Delta v^{RX} (p = 0.1 MPa) / cm^3 mol^{-1}$	6.03 ± 0.31	2.86 ± 0.13			
$\Delta v^{HP} (p = 0.1 MPa) / cm^3 mol^{-1}$	—	2.75 ± 0.17^e	4.05 ± 0.24^e	1.19 ± 0.09^e	2.89 ± 0.35^e
$(dT/dp)^{CC} / K MPa^{-1}$	0.299 ± 0.030 (0.287^c)	0.365 ± 0.044 (0.365^c)	0.221 ± 0.024	0.666 ± 0.113	0.344 ± 0.065
$(dT/dp)^{exp} / K MPa^{-1}$	0.320 ± 0.032	0.303 ± 0.020	0.208 ± 0.005	0.681 ± 0.032	0.380 ± 0.021

^a Volume changes determined from X-ray powder diffraction measurements (Δv^{RX}) and from extrapolation at normal pressure of the high-pressure measurements (Δv^{HP}), slope of the pressure–temperature two-phase equilibria derived from the application of the Clausius–Clapeyron equation (dT/dp^{CC}) and read from pT diagram (dT/dp^{exp}) of the CBr_2Cl_2 . ^b Values obtained by extrapolation of the [M + R], [R + FCC] and [R + L] equilibria of the $CCl_4 + CBr_2Cl_2$ and $CBrCl_3 + CBr_2Cl_2$ two-component systems.¹⁷ ^c Using the enthalpy values from Otha *et al.*¹⁵ ^d Extrapolated from the p – T phase diagram. ^e From extrapolation at normal pressure of the high-pressure measurements.

scattering,¹⁶ densitometry,²⁰ infrared and Raman spectroscopy,²¹ dielectric spectroscopy²² and the pressure–temperature phase diagram has been recently established.¹⁴

As for CBr_2Cl_2 the polymorphism at ordinary pressure consists of two stable forms in the solid state.^{16,23} At *ca.* 259 K, the low-temperature phase transforms to an OD face centred-cubic (FCC) phase, stable up to the melting point (294 K). Thermodynamic properties have been determined by means of adiabatic calorimetry from 5 to 300 K (enthalpy changes and temperatures are collected in Table 1).¹⁵

According to the molecular similarity between CBr_2Cl_2 and $CBrCl_3$ with that of CCl_4 , the structures of the low-temperature phases were attempted by Brinbrek *et al.* on the basis of the structural model of CCl_4 and CBr_4 ($C2/c$, $Z = 32$).¹⁶ For the “ordered” phases of $CBrCl_3$ and CBr_2Cl_2 compounds the molecules were assumed to be disordered so that sites have fractional occupancies of 0.75 and 0.25, for $CBrCl_3$, and 0.50, for CBr_2Cl_2 , for each of Cl and Br atoms, respectively. Thus, all the low-temperature phases were found to be isostructural.¹⁶ The isomorphism relationship between the stable low-temperature monoclinic phases of CBr_2Cl_2 , $CBrCl_3$ and CCl_4 has been put into evidence throughout the continuous evolution of the lattice parameters for the whole range of composition for the $CBrCl_3 + CBr_2Cl_2$ and $CCl_4 + CBr_2Cl_2$ two-component systems.¹⁷

The sketch of these binary systems is depicted in Fig. 1. The systems show the isomorphism relationship between the stable OD FCC phases of $CBrCl_3$ and CBr_2Cl_2 . It should be noticed the existence of a [R + FCC] equilibrium, whatever the system, which interferes with the low-temperature equilibrium between the low-temperature monoclinic ($C2/c$) phase and the OD R and FCC phases. A thermodynamic assessment of the involved equilibria, conducted by means of the concept of crossed isopolymorphism,¹³ coherently reproduced all the involved equilibria and provided a coherent set of data for the thermodynamic properties (enthalpy changes and temperatures) of non-experimentally available phase transitions of pure compound CBr_2Cl_2 which enables to infer the existence of a *virtual* rhombohedral phase for such compound.

Extrapolated equilibria in Fig. 1 evidence the existence of M to R ($T^{M-R} = 262.0 \pm 2.0$ K) and R to FCC ($T^{R-FCC} = 243.6 \pm 2.0$ K) phase transitions, from both systems, and R to L ($T^{R-L} = 280.7 \pm 2.0$ K), from the $CCl_4 + CBr_2Cl_2$ system. According to the mole fraction variation of the enthalpy change for the [R + L] and [R + FCC] equilibria, the inferred values for the CBr_2Cl_2 compound relating the *virtual* R phase were $\Delta_R^L H = (2.36 \pm 0.15)$ kJ mol^{−1}, $\Delta_R^{FCC} H = (0.436 \pm 0.080)$ kJ mol^{−1}, and $\Delta_M^R H = (4.80 \pm 0.22)$ kJ mol^{−1}. By the same procedure, the inferred lattice parameters for the R phase of CBr_2Cl_2 compound were $a^R = 14.772(15)$ Å, $\alpha^R = 89.44(2)^\circ$ at 243.2 K ($v^R = 92.4 \pm 0.5$ cm³ mol^{−1}). Owing to the fact that phase R does not exist, at ordinary pressure, its stability domain, if any, should appear in the high-pressure region and transition temperatures obtained from the extrapolation of the two-phase equilibria should acquire physical meaning and be topologically coherent with two-phase equilibria of the pressure–temperature phase diagram of CBr_2Cl_2 .

The purpose of this paper is then to report on the polymorphism of CBr_2Cl_2 compound as a function of temperature

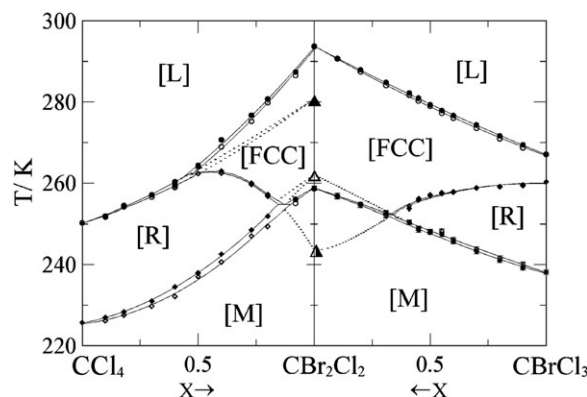


Fig. 1 Experimental equilibria (points and continuous lines) and extrapolated equilibria (dotted lines) obtained by means of thermodynamic assessment of the two-component systems.¹⁷ Triangles at $X = 1$ account for the non-experimentally available transitions for CBr_2Cl_2 (▲, R–FCC; △, M–R; ▴, R–L).

and pressure. It will be unambiguously demonstrated the existence of a high-pressure region in which the “missing” rhombohedral R phase for this compound is stable. In addition, the “glassy features” related to the freezing of exchange positions between Cl and Br atoms between the monoclinic sites will be analyzed and compared with those previously found for the isomorphous phase of CBrCl_3 .¹⁴

2 Experimental

2.1 Samples

CBr_2Cl_2 was purchased from Aldrich with a purity grade of 98% and was fractionally distilled, the final compound showing a melting temperature which agrees with that reported in previous works.

2.2 Equipment at ordinary pressure

Thermal analysis. Thermal analysis was carried out by means of a Perkin-Elmer DSC-7 instrument equipped with a homemade low-temperature device using a scanning rate of 2 K min^{-1} and *ca.* 15 mg sample masses hermetically sealed into high-pressure stainless steel pans under a nitrogen flux.

Density. The density of the liquid state at normal pressure from 295 to 343 K (with uncertainties of *ca.* $5 \times 10^{-5} \text{ g cm}^{-3}$) were carried out by means of an Anton Paar D5000 densimeter with temperature stability of $\pm 0.02 \text{ K}$. Bidistilled water and *n*-hexane (99.9%) were used for calibration, the density values taken from literature.^{24,25}

X-Ray diffraction. High-resolution X-ray powder diffraction measurements using the Debye–Scherrer geometry and transmission mode were performed with a horizontally mounted INEL cylindrical position-sensitive detector (CPS-120) made of 4096 channels ($0.029^\circ 2\theta$ angular step).²⁶ Monochromatic $\text{Cu-K}\alpha_1$ ($\lambda = 1.54056 \text{ \AA}$) radiation was selected by means of an asymmetrically focusing incident-beam curved quartz monochromator. The generator power was set to 40 kV and 25 mA. Low-temperature measurements were performed by means of a liquid nitrogen 600 series Cryostream Cooler from Oxford Cryosystems.

External calibration by means of cubic phase $\text{Na}_2\text{Ca}_3\text{Al}_2\text{F}_4$ was applied for channels to be converted into 2θ -degrees by means of cubic spline fittings.²⁷ The peak positions were determined by pseudo-Voigt fittings.

Liquid samples were introduced into 0.1 mm diameter Lindemann capillaries which were rotated around their axes during data collection to improve averaging of the crystallites.

Patterns were recorded on heating every 10 K in the temperature range of 90–255 K and every 5 K from this temperature up to the melting point, with acquisition times of at least 120 min for the low-temperature monoclinic phase and 60 min for the high-temperature OD FCC phase. Stabilization times of at least 10 min at each temperature before the data acquisition were preset.

PEAKOC application from DIFFRACTINEL software was used for the calibration as well as for the peak position determinations after pseudo-Voigt fittings. For indexing pur-

poses as well as Rietveld refinement, Material Studio program was used.²⁸

2.3 Equipment at high-pressure

Density. High-pressure density values were determined by means of a home-made *pVT* apparatus (uncertainty of *ca.* $10^{-4} \text{ g cm}^{-3}$) coming from the high-pressure laboratory of Prof. Dr A. Würflinger (Ruhr-Universität, Bochum, Germany). Density data are taken at increasing and decreasing pressure in order to correct the possible hysteresis produced by the friction of the displacement of a piston. The change of the volume is done inductively with a ferromagnetic wire inserted into a coil. Calibration was performed using hexane as a reference substance. Details of the experimental system as well as the procedure have been detailed elsewhere.^{29,30}

High-pressure neutron powder diffraction. Some high-pressure patterns were collected using the D1B diffractometer at the Institut Laue-Langevin (Grenoble), using a wave length of $\lambda = 2.52 \text{ \AA}$, as determined by calibration using a TiO_2 sample. Low-resolution patterns ($0.20^\circ 2\theta$ angular step) in the 5–80 2θ -degrees were obtained in the 280–320 K temperature domain using an *Orange* cryostat. Liquid samples were introduced in clamp-type cells equipped with a piston-cylinder design for which pressure was initially selected by means of a hydraulic press. Two samples with pressures about 80 ± 15 and $150 \pm 30 \text{ MPa}$ were prepared. Data analysis for the patterns was conducted in an analogous way that for those obtained at normal pressure.

3 Results

Patterns of the low-temperature monoclinic phase were submitted to Rietveld profile refinement by means of the “powder refinement” option of the Material Studio program. Atomic coordinates of the four molecules in the asymmetric unit of CBr_4 ,³¹ were used as initial parameters. The fractional occupancies of the halogen sites were set as 0.5 for both Br and Cl atoms, and rigid body representing a pseudo-molecule with tetrahedral symmetry for the bond angles in which overlapping Br and Cl atoms located at 1.939 and 1.772 Å from the central carbon atom C, respectively, was used. Fig. 2 shows the experimental and calculated profiles, together with the difference between them, at 220.2 and 90.2 K (see details in ESI†). The monoclinic lattice ($C2/c$, $Z = 32$) parameters of CBr_2Cl_2 agree quite well with those previously published for the whole temperature range (see Fig. 3).¹⁶ It should be mentioned that any anomaly at the glass transition temperature (*ca.* 90 K) is observed. In addition, in spite of the high-resolution of the diffraction patterns, we did not detect any ordering of the Cl and Br atoms (checked by varying the fractional occupancies as a function of temperature). This experimental aspect agrees with the fact that the glass transition is a purely dynamic crossover and due to the long-range positional order, the freezing of the disorder produced by the exchange of the halogen atoms does not have any noticeable influence on the patterns, which are in fact obtained as space and time averages.

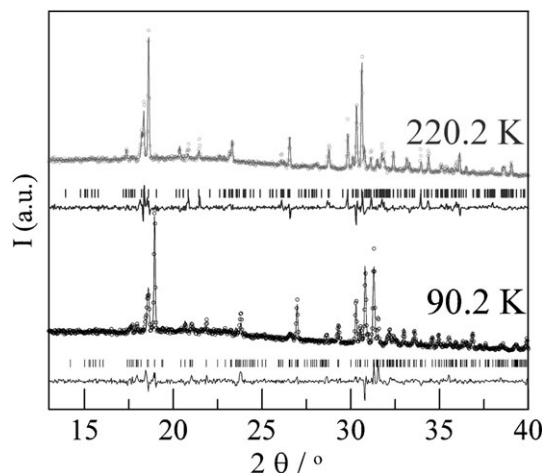


Fig. 2 Experimental (○) and theoretical (—) diffraction patterns of low-temperature monoclinic phase ($C2/c$, $Z = 32$) for CBr_2Cl_2 at 90.2 K (bottom, $R_p = 6.7$; $R_{wp} = 9.2$) and at 220.2 K (top, $R_p = 7.1$; $R_{wp} = 9.9$) along with the difference profiles (lower curves) and Bragg reflections (vertical bars) ($\lambda = 1.5406 \text{ \AA}$).

The collected lattice parameters for the monoclinic phase together with those for OD FCC phase and density measurements for the liquid phase were used to calculate the molar volume as a function of temperature and, from them, the

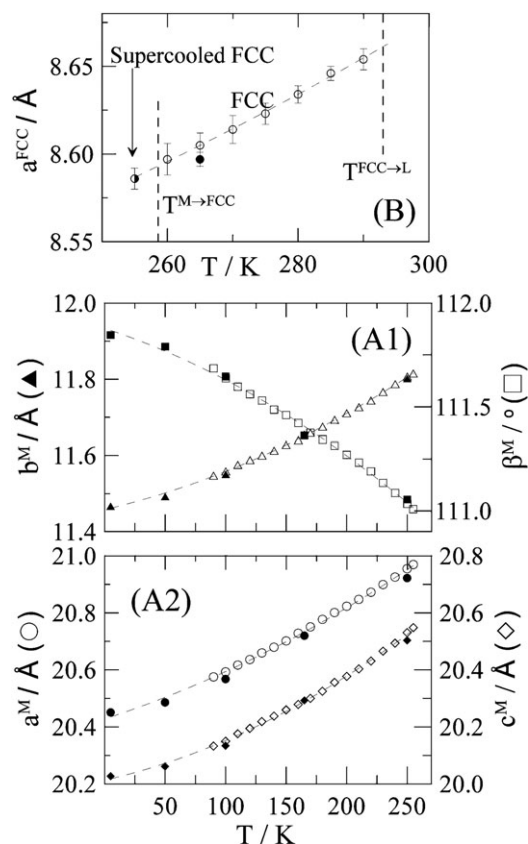


Fig. 3 Lattice parameters of CBr_2Cl_2 for the low-temperature monoclinic (A) and the for OD FCC (B) phases as a function of temperature. Full symbols correspond to refs. 16 and 23 while half-full circle corresponds to the supercooled FCC OD phase.

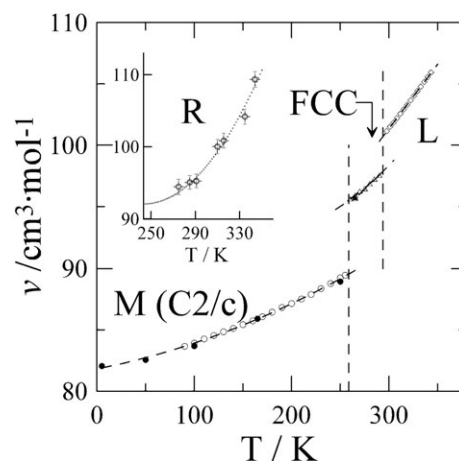


Fig. 4 Molar volume of CBr_2Cl_2 as a function of temperature at normal pressure. Full symbols for solid phases were obtained from literature.^{9,16} Inset: values of the normal-pressure molar volumes of the high-pressure rhombohedral phase obtained by extrapolation at $p = 0.1 \text{ MPa}$ from the isotherms measured as a function of pressure (see Fig. 5).

volume variations (at ordinary pressure) at the solid–solid and melting transitions (Fig. 4).

As far as high-pressure density measurements are concerned, several representative isotherms are sketched in Fig. 5. These results were used to build up the pressure–temperature phase diagram, which is shown by the top inset in Fig. 5, as well as to derive the volume changes as a function of pressure (Fig. 6). It should be noticed that a new high-pressure phase appears and thus two triples points sharing the three solid phases ($[M + FCC + R]$ at 33.0 MPa, 269.4 K) and the OD and liquid phases ($[FCC + R + L]$ at 104.1 MPa, 320.9 K) emerge. As we will demonstrate, the high-pressure phase is the “missing” rhombohedral phase for this member of the halogenomethane series ($CBr_{4-n}Cl_n$, $n = 0, \dots, 4$). Moreover, it is worth to notice that the appearance of the new

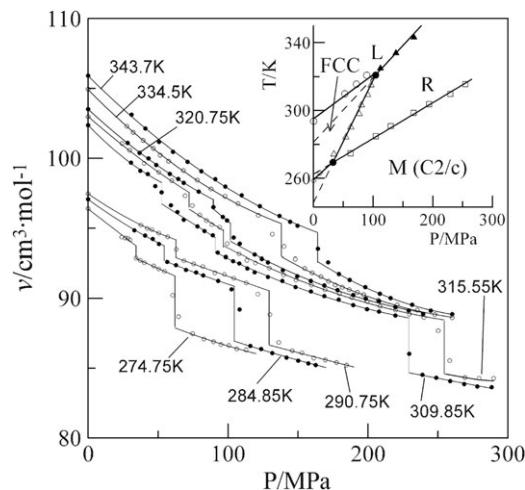


Fig. 5 Molar volume as a function of pressure for several temperatures and, as an inset, pressure–temperature phase diagram for CBr_2Cl_2 . Dashed lines correspond to the extrapolation of two-phase equilibria at ordinary pressure.

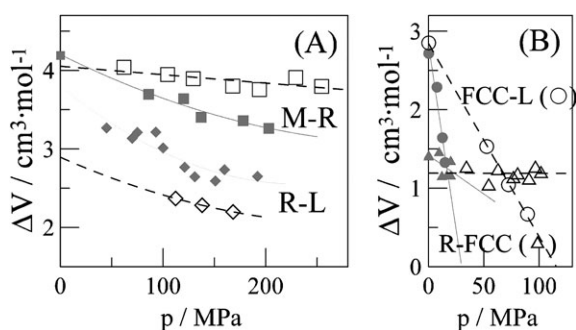


Fig. 6 Volume changes as a function of pressure for the phase transitions M–R and R–L (A) and R–FCC and FCC–L (B) of CBr_2Cl_2 (empty symbols) derived from pVT measurements. Full grey symbols correspond to values of CBrCl_3 from ref. 7.

R phase is concomitant with the disappearance of the FCC phase at high pressure.

Fig. 7 shows the measured neutron diffraction pattern together with that calculated for the R phase for CBr_2Cl_2 at 300 K and *ca.* 80 MPa along with the difference profile. It should be noticed that indexing of neutron diffraction patterns by using standard procedures fell short of indexing the new rhombohedral phase because reflections are closely spaced and, thus, many of them overlap (see the vertical bars showing the possible reflections in Fig. 7). Then, although the low-resolution of the neutron scattering measurements at high pressure (due to the D1b diffractometer) made impossible to perform an irreproachable Rietveld refinement, a model built up by mimicking the rhombohedral phases of CCl_4 and CBrCl_3 is found to be able to reproduce the pattern, thus concluding that the symmetry of the new high-pressure phase is that of the rhombohedral phases found for the members of the halogenomethane series. The pattern matching of Fig. 7 evidences the last conclusion.

Fitted lattice parameters are found to be about $a^{\text{R}} \approx 14.6 \pm 0.3$ Å and $\alpha \approx 89.2 \pm 0.2^\circ$, which, taking into account the

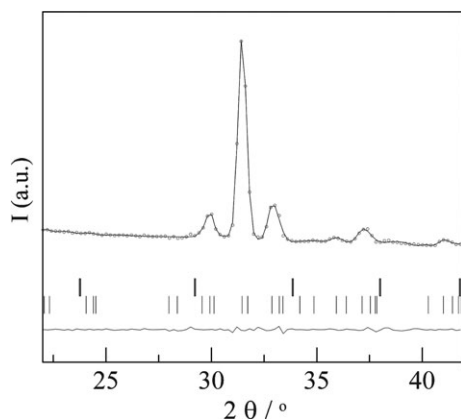


Fig. 7 Experimental (circles) and calculated (continuous line, $a^{\text{R}} = 14.6$ Å) neutron diffraction patterns of the rhombohedral phase for CBr_2Cl_2 at 300 K and *ca.* 80 MPa along with the difference profile (bottom line). The vertical bars stand for the Bragg reflections ($\lambda = 2.52$ Å) of the R phase (bottom vertical lines) and a FCC lattice isostructural ($a^{\text{FCC}} = 8.65$ Å) to that at normal pressure (top vertical lines) for CBr_2Cl_2 .

experimental error limits, gives rise to a volume close to that obtained by means of high-pressure density measurements for the R phase. The same figure displays the Bragg reflections for the FCC phase of CBr_2Cl_2 providing evidence that pattern does not match with such symmetry.

Finally, results obtained from the calorimetric measurements, temperatures and enthalpy changes, are summarized in Table 1 together with those reported by Ohta *et al.* obtained from adiabatic calorimetry.¹⁵ Agreement between both series of results, within the experimental error, is evidenced. The table contains also volume changes and experimental and calculated (by means of the Clausius–Clapeyron equation) two-phase equilibrium slopes.

4 Discussion

From the two-phase equilibria of the two-component systems $\text{CCl}_4 + \text{CBr}_2\text{Cl}_2$ and $\text{CBr}_2\text{Cl}_2 + \text{CBrCl}_3$ (Fig. 1) the non-experimentally available (at normal pressure) transition temperatures relating phase R can be inferred (see Table 1).¹⁷ These “virtual” temperatures make its natural appearance and acquire real physical significance when the two-phase equilibria of the pressure–temperature phase diagrams are analyzed. As is shown up in Table 1, the M to R and R to FCC transition temperatures, as well as the melting of the R phase obtained from the two methods, is virtually the same, within the experimental error limits. Full coherence is also obtained when values of volume change are compared and put into the Clausius–Clapeyron equation to evaluate the slopes of the two-phase equilibria. The most, even surprising, relevant experimental fact concerns the comparison of the extrapolated molar volume at normal pressure for the high-pressure R phase. From the extrapolation to 0.1 MPa of the high-pressure molar volumes of the R phase (see Fig. 5) for each isotherm and subsequent fitting of such values as a function of temperature (see inset in Fig. 4), a value of $v^{\text{R}}(243.2 \text{ K}, 0.1 \text{ MPa}) = (92.1 \pm 0.5) \text{ cm}^3 \text{ mol}^{-1}$ is obtained, which compares more than well with the value obtained from the analysis of the lattices parameters variation as a function of mole fraction at 243.2 K for the two-component system $\text{CCl}_4 + \text{CBr}_2\text{Cl}_2$ ($92.4 \pm 0.5 \text{ cm}^3 \text{ mol}^{-1}$).¹⁷

As far as the volume changes as a function of pressure are concerned, special relevance comes from those of the melting of the FCC phase (see Fig. 6(B)). It can be seen that such a change vanishes at the [FCC + R + L] triple point (104.1 MPa, 320.9 K) and that, although there is not a thermodynamic reason for such a behaviour, it is noticeable that the same behaviour was found for the volume variation as a function of pressure for the CBrCl_3 compound (at 30.7 MPa, 278.8 K) for the same transition (see grey symbols on the same figure).¹⁴ This result necessarily implies, according to the Clausius–Clapeyron equation, that the related enthalpy change must also vanish when approaching the triple point.

As for the “missing” transitions at normal pressure (M to R, R to FCC and R to L), the volume changes as a function of pressure can be extrapolated at $p = 0.1$ MPa (see dashed curves in Fig. 6) and replaced into the Clausius–Clapeyron equation $(dT_c/dp)^{\text{CC}}$, together with the enthalpy changes obtained from the extrapolation of the enthalpy data as a

Table 2 Polynomial equations $p = p_0 + p_1T + p_2T^2$ (T in K and p in Å or in degrees for β parameter) to which the lattice parameters were fitted as a function of temperature and molar volume (v in $\text{cm}^3 \text{mol}^{-1}$) for the liquid phase. R is the reliability factor, defined as $R = \sum(p_{\text{exp}} - p_c)^2/p_c^2$, where p_{exp} and p_c are the measured and calculated lattice parameters, respectively. A three-parameter polynomial equation for the molar volume of the liquid phase is also given

Phase	Temperature range/K	Parameter	p_0	$10^3 p_1$	$10^5 p_2$	$10^6 R$
II (C2/c)	5–250	$a/\text{\AA}$	20.428(10)	1.4(1)	0.29(5)	6.3
		$b/\text{\AA}$	11.458(3)	0.74(5)	0.26(1)	2.0
		$c/\text{\AA}$	20.013(7)	0.96(10)	0.43(3)	3.1
		$\beta/^\circ$	111.88(1)	−1.9(2)	−0.58(6)	0.4
I (FCC)	255–294	$a/\text{\AA}$	8.460(27)	−0.78(2)	0.5(3)	0.1
L	295–343	$v/\text{cm}^3 \text{mol}^{-1}$	82.857(35)	23.8(2)	12.7(3)	0.003

function of composition for the two-component systems¹⁷ and compared with the experimental value, $(dT_c/dp)^{\text{exp}}$, obtained from the pressure–temperature diagram. Results listed in Table 1 evidence that there is a good agreement independently of the experimental availability at normal pressure of the phase transition.

Then, the complete set of independent experimental data puts in evidence that the new observed high-pressure phase is the “common” rhombohedral phase observed for some halogenomethane compounds ($\text{CBr}_{4-n}\text{Cl}_n$) at normal pressure and also for all the methylchloromethane compounds ($\text{C}(\text{CH}_3)_{4-n}\text{Cl}_n$) at normal ($n = 2, 3, 4$)^{12–13,32,33} or high pressure ($n = 0, 1$).³⁴

To obtain information about the intermolecular interactions, lattice parameters obtained for the monoclinic phase were fitted as a function of temperature (Table 2) and the isobaric thermal-expansion tensor was calculated. The deformation of the lattice by a change in the temperature is minimal in the directions of the highest atomic density, *i.e.* in the directions of the highest intermolecular interactions. For short, the principal axes of the isobaric thermal expansion tensor allows to determine the directions of the weakest and highest deformation (commonly referred to as hard and soft directions, respectively)^{35,36} related to the directions of the corresponding intermolecular interactions in the crystal structure.

The tensor for the monoclinic phase is unequivocally defined by the principal coefficients α_1 , α_2 and α_3 , and by an angle between one of the principal directions (α_3) and the crystallographic axis *a*. According to the Newman principle, the α_2 axis is coincident with the 2-fold axis *b* of the crystal. Details of the procedure to calculate the tensor by means of the program DEFORM³⁷ have been detailed elsewhere.³²

The variations of the principal coefficients with the temperature are plotted in Fig. 8(A) and, as an inset, the three-dimensional thermal expansion tensor at 180 K along its principal axes together with the direction of the crystallographic axes is sketched. As for the homologous phase of CBrCl_3 compound (see grey lines in Fig. 8(A)), the hardest direction is found along the α_3 direction. Fig. 8(B) and (C) provide additional evidences for the unambiguous similarity of the thermal expansion between CBr_2Cl_2 and CBrCl_3 compounds in the monoclinic as well as in the OD FCC and liquid phases.

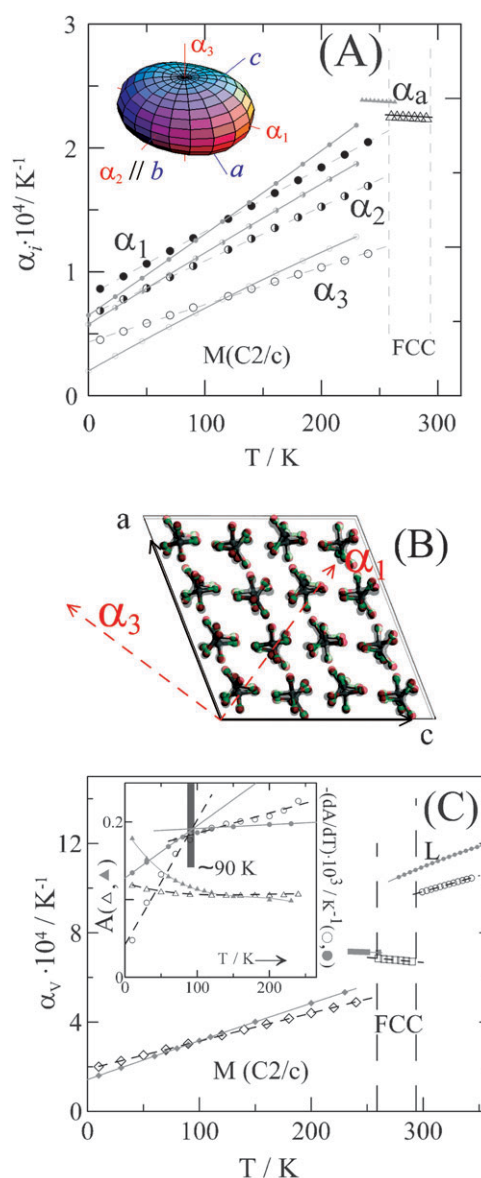


Fig. 8 (A) The α_i principal coefficients as a function of temperature for CBr_2Cl_2 for the low-temperature monoclinic phase (circles) (α_2 is chosen parallel to the crystallographic direction (*b*) and for the FCC phase (triangles). Inset depicts the thermal-expansion tensor of monoclinic phase at $T = 180 \text{ K}$ in the frame of the principal directions α_i (dotted red lines) together with the crystallographic axes (continuous blue lines). The full length of the α_i axes corresponds to $2.0 \times 10^{-3} \text{ K}^{-1}$. (B) Projection of the monoclinic structure of CBr_2Cl_2 superimposed to that of CBrCl_3 (grey) on the (0*k*0) crystallographic plane. (C) The volume expansivity ($\alpha_v = \alpha_1 + \alpha_2 + \alpha_3$) as a function of temperature. As an inset, the asphericity index (*A*) and its derivative (dA/dT) as a function of the temperature for the low-temperature monoclinic phase are shown. Dashed area indicates the change of the slope (ca. 90 K) for the derivative of the asphericity index. Grey symbols in all cases correspond to the values of CBrCl_3 .¹⁴

As far as the anisotropy of the thermal expansion tensor in the monoclinic phase is concerned and, in particular, related to the reported glass transition at 90 K,¹⁵ the results deserve a special comment. It is well-known that continuous variation of the molar volume against temperature as well as the

discontinuity in the volume expansivity are irrefutable signatures of the existence of the canonical glass transition. Nevertheless, as is evidenced by Fig. 8(C), glass transition is not shown by any discontinuity at around 90 K but only by the numerical derivative of the asphericity coefficient (inset in Fig. 8(C)). This coefficient, defined as $A = (2/3)[1 - (3\beta/\alpha_v^2)]^{1/2}$, where $\beta = \alpha_1\alpha_2 + \alpha_2\alpha_3 + \alpha_1\alpha_3$, accounts for and enhances the anisotropy of the intermolecular interactions. The result was previously found for the glass transition of CBrCl_3 (results are displayed also in the inset of Fig. 8(C) by means of grey symbols) and was postulated as a possible signature of the glass transition.¹⁴ It seems, then, that such a particular glass transition, associated with the freezing of exchange positions between Cl and Br atoms, and thus with the frustration of the ordering of the weak molecular dipoles, is controlled by a competition between intermolecular potential and the potential barrier hindering the molecular reorientation.

Concerning the isotropic thermal expansivity of the OD FCC phase it can be concluded (see Fig. 8(A) and (C)) that it behaves like that of the isomorphous phase of CBrCl_3 .

5 Conclusions

By combining a wide set of experimental techniques at normal as well as at high pressure, we have firmly determined the properties of the different phases, and their transitions, as a function of temperature and pressure for CBr_2Cl_2 . Moreover, we have provided evidences for the existence of an orientationally disordered rhombohedral phase, for which the stability pressure–temperature domain has been unambiguously established. The existence of this phase for the analyzed material makes still more uniform the series of the halogenomethane compounds ($\text{CBr}_{4-n}\text{Cl}_n$). The thermodynamic high-pressure data show the existence of two triple points, [M + FCC + R] at (33.0 MPa, 269.4 K) and [FCC + R + L] at (104.1 MPa, 320.9 K), which in fact define the limits of stability of the OD FCC phase. It is noteworthy that for both CBr_2Cl_2 and CBrCl_3 materials, the FCC-L volume change vanishes at the [FCC + R + L] triple point, without any aprioristic thermodynamic reason. As a consequence, enthalpy change for the melting of the FCC phase must also vanish when approaching the triple point.

Interesting conclusions can be drawn from the close behaviour of the derivative analysis of asphericity index as a function of the temperature for the monoclinic phase. The present work confirms the proposal previously reported¹⁴ concerning the change of such a parameter for the glass transition related to the freezing of exchange positions between Cl and Br atoms.

We would like to point out that the family of halogenomethane compounds constitutes a very interesting case because molecules with very close symmetry and size, with both nonpolar (CCl_4 and CBr_4) and slightly polar (CBrCl_3 and CBr_2Cl_2) species, give rise to a different polymorphic behaviour when only the temperature variable is considered at ordinary pressure. Thus, for such a limited vision, the number and symmetry of the appearing phases seemed to be uncorrelated. Nevertheless, when the “real” phase-space governed by two variables, temperature and pressure, is scanned, poly-

morphic behaviour of a family can be rationalized in terms of common topological pressure–temperature phase diagrams.

Finally, another aspect of this work that should deserve a special comment concerns the generalities of the thermodynamic paths we have used in this work. Pressure–temperature landscape is not yet a typical thermodynamic landscape scenario in which polymorphism is described, in spite of real advances of technology to get high-pressure conditions.^{3,8} Understanding pressure–temperature polymorphism among “simple” molecular compounds such as those analysed here to establish proper thermodynamic basis is still a “pressing” need.

Acknowledgements

This work was supported by grants FIS2005-00975, Spain, and 2005SGR-00535, Catalonia. The authors wish to thank Dr S. Coco from the Chemical Physics Department, University of Valladolid, for purifying the CBr_2Cl_2 samples used in this work as well as the high-pressure technical service at the ILL Institute for its support with the measurements.

References

- 1 F. P. A. Fabbiani and C. R. Pulham, *Chem. Soc. Rev.*, 2006, **35**, 932.
- 2 P. F. McMillan, *Chem. Soc. Rev.*, 2006, **35**, 855.
- 3 P. F. McMillan, *Nat. Mater.*, 2005, **4**, 715.
- 4 A. San-Miguel, *Chem. Soc. Rev.*, 2006, **35**, 876.
- 5 M. C. Wilding, M. Wilson and P. F. McMillan, *Chem. Soc. Rev.*, 2006, **35**, 943.
- 6 M. I. McMahon and R. J. Nelmes, *Chem. Soc. Rev.*, 2006, **35**, 964.
- 7 A. F. Goncharov and R. J. Hemley, *Chem. Soc. Rev.*, 2006, **35**, 899.
- 8 P. F. McMillan, *Nat. Mater.*, 2007, **6**, 7.
- 9 A. Włodarczyk, P. F. McMillan and S. A. Greenfield, *Chem. Soc. Rev.*, 2006, **35**, 890.
- 10 J. Bernstein, in *Polymorphism in Molecular Crystals*, IUCr Monographs on Crystallography, Clarendon Press, Oxford, 2002.
- 11 H. G. Brittain, *J. Pharm. Sci.*, 2002, **91**, 1573.
- 12 R. Rudman and B. Post, *Science*, 1966, **154**, 1009.
- 13 L. C. Pardo, M. Barrio, J. Ll. Tamarit, D. O. López, J. Salud, Ph. Negrier and D. Mondieig, *Phys. Chem. Chem. Phys.*, 2001, **3**, 2644.
- 14 B. Parat, L. C. Pardo, M. Barrio, J. Ll. Tamarit, Ph. Negrier, J. Salud, D. O. López and D. Mondieig, *Chem. Mater.*, 2005, **17**, 3359.
- 15 T. Ohta, O. Yamamuro and T. Matsuo, *J. Phys. Chem.*, 1995, **99**, 2403.
- 16 O. S. Binbrek, S. E. Lee-Dadswell, B. H. Torrie and B. M. Powell, *Mol. Phys.*, 1999, **96**, 785.
- 17 M. Barrio, Ph. Negrier, J. Ll. Tamarit, L. C. Pardo and D. Mondieig, *J. Phys. Chem. B*, 2007, **111**, 8899.
- 18 L. C. Pardo, R. Rey, E. Llanta, K. Ando, D. O. López, J. Ll. Tamarit and M. Barrio, *J. Chem. Phys.*, 2000, **112**, 7505, and references therein.
- 19 N. Veglio, F. J. Bermejo, L. C. Pardo, J. Ll. Tamarit and G. J. Cuervo, *Phys. Rev. E*, 2005, **72**, 031502, and references therein.
- 20 C. Jarne, M. Artal, J. Muñoz-Embid, I. Velasco and S. Otín, *Can. J. Chem.*, 1999, **77**, 2046.
- 21 Y. S. Park and H. F. Shurvell, *Can. J. Spectrosc.*, 1988, **33**, 38.
- 22 R. C. Miller and C. P. Smyth, *J. Chem. Phys.*, 1956, **24**, 814.
- 23 S. E. Lee-Dadswell, B. H. Torrie, O. S. Binbrek and B. M. Powell, *Physica B*, 1998, **241–243**, 459.
- 24 S. L. Randzio, J.-P. E. Grolier, J. R. Quint, D. J. Eatough, E. A. Lewis and L. D. Hansen, *Int. J. Thermophys.*, 1994, **15**, 415.

- 25 F. I. Mopsik, *J. Res. Natl. Bur. Stand., Sect. A*, 1967, **71**, 287.
- 26 J. Ballon, V. Comparat and J. Poux, *Nucl. Instrum. Methods*, 1983, **217**, 213.
- 27 M. Evain, P. Deniard, A. Jouanneaux and R. Brec, *J. Appl. Crystallogr.*, 1993, **26**, 563.
- 28 MS Modeling (Material Studio) 3.0 software http://www.accelrys.comcom/mstudio/ms_modeling.
- 29 A. Würflinger, A. M. Sandmann and W. Weissflog, *Z. Naturforsch., Teil A*, 2000, **55**, 823.
- 30 R. Landau and A. Würflinger, *Rev. Sci. Instrum.*, 1980, **66**, 533.
- 31 M. More, F. Baert and J. Lefebvre, *Acta Crystallogr., Sect. B*, 1977, **33**, 3681.
- 32 P. Negrier, L. C. Pardo, J. Salud, J. Ll. Tamarit, M. Barrio, D. O. López, A. Würflinger and D. Mondieig, *Chem. Mater.*, 2002, **14**, 1921.
- 33 L. C. Pardo, M. Barrio, J. Ll. Tamarit, J. Salud, D. O. López, P. Negrier and D. Mondieig, *Phys. Chem. Chem. Phys.*, 2004, **6**, 417.
- 34 M. Barrio, P. de Oliveira, R. Céolin, D. O. López and J. Ll. Tamarit, *Chem. Mater.*, 2002, **14**, 851.
- 35 J. Ll. Tamarit, D. O. López, X. Alcobe, M. Barrio, J. Salud and L. C. Pardo, *Chem. Mater.*, 2000, **12**, 555.
- 36 J. Salud, M. Barrio, D. O. López, X. Alcobe and J. Ll. Tamarit, *J. Appl. Crystallogr.*, 1998, **31**, 748.
- 37 A. Filhol, J. Lajzerowicz and M. Thomas, *DEFORM program*, unpublished software, 1987.